Journal of Applied Fluid Mechanics, Vol. 11, No. 5, pp. 1247-1253, 2018.
Available online at www.jafmonline.net, ISSN 1735-3572, EISSN 1735-3645.
DOI: 10.29252/jafm.11.05.28588

Experimental and CFD Study of Internal Flow inside a Sessile Microdroplet undergoing Lateral Vibration

T. Zhu[1,2,4,5,*], Z. Zhao[3,*], L. Lv,[2] W. Chen [1,4,5] and L. Dong[1,2,4,5†]

[1] *School of Chemistry and Chemical Engineering, Chongqing University, Chongqing, 40004, PR China*

[2] *School of Chemistry and Chemical Engineering, Collaborative Innovation Center for Green Development in Wuling Moutain Area, Research Center for Environmental Monitoring, Hazard Prevention of Three Gorges Reservoir, Yangtze Normal University, Fuling 408100, Chongqing, PR China*

[3] *Qingdao Institute of Bioenergy and Bioprocess Technology, Chinese Academy of Sciences, Qingdao, Shandong, 266101, PR China*

[4] *National-Municipal Joint Engineering Laboratory for Chemical Process Intensification and Reaction, Chongqing University*

[5] *Chongqing Univ, Key Lab Low Grade Energy Utilizat Technol & Syst, Minist Educ, Chongqing, PR China*

† *Corresponding Author Email: Lcdong72@cqu.edu.cn*
* *T. Zhu and Z. Zhao contributed equally to this work.*

(Received November 14, 2017; accepted February 3, 2018)

ABSTRACT

In this study, the internal flow pattern of a sessile microdroplet undergoing a lateral vibration was analyzed by using both the experimental and CFD simulation methods. By initially staining the droplet partially with fluorescent dye, the main flow inside the laterally vibrating microdrop was experimentally demonstrated to be that the main fluid flows downward along the central axis and ascends upward along the surface to form two counterflow circuits. Experimental evaluation of fluid mixing inside the droplets verified that the internal flowing velocity is dependent on the vibrating frequency, the main fluid flows faster at the resonant modes. CFD simulation using the VOF-CSF model showed that extra flow circuits exit inside the oscillating droplet besides the main flow. The diffusion of substrate momentum within the Stokes layer results in the two flow circuits near the bottom substrate, and the Laplace force due to the droplet deformation induces the two counter-current flow circuits near the surfaces of the microdroplet.

Key words: Internal flow; Sessile drop; Lateral vibration; Microdrops.

1. INTRODUCTION

In recent years, the behavior of sessile liquid droplets in partial contact with a solid substrate actuated by external actuators and energy sources, e.g. the mechanical vibration and induced electrowetting, has been studied extensively not only for scientific purpose but also for industrial applications. Among the various methods for manipulating the liquid droplets, driving droplet vibration by a periodic force at the resonant frequencies has attracted considerable interests due to the applications in the technological processes, such as heating, ventilation, air conditioning and extraction (Wilkes and Basaran, 1997; Moon *et al*., 2006; Lee *et al*., 2015; Daw and Finkelstein, 2006). Kelvin (1882) and Rayleigh (1894) have employed the pioneer studies of the oscillation of free liquid droplets. Lamb (1932) obtained the general equation (Lamb's equation) for the different resonant frequencies of a free liquid drop. Later analysis by Strani and Sabetta (1984) showed that when a droplet is contacted with a solid surface, the resonant oscillating frequencies of the droplet could be raised slightly. Their study also demonstrated that the sessile droplet has a low-frequency mode (rocking mode) besides the Rayleigh modes calculated by Lamb's equation. When a sessile droplet stands on a vibrating hydrophobic substrate, the contact line remains pinned at low vibration amplitudes, whereas at higher amplitudes, the

contact line experiences an oscillatory motion by overcoming the contact angle hysteresis. Noblin *et al*. (2009a) studied the vertical vibration of a water drop standing on a hydrophobic substrate, showing that the drops experience a stick-slip motion at high vibration amplitudes. They also studied the motion of a drop lying on a plate simultaneously submitted to horizontal and vertical harmonic vibrations, offering new possibilities of controlled motion in droplet microfluidics applications. Brunet *et al*. (2008; 2009) realized the upward motion of liquid drops against gravity on an inclined plate undergoing a vertical vibration. Rahimzadeh and Eslamian (2017) studied the effect of imposing ultrasonic vibration on the oscillations and evaporation of sessile droplets. The stick-slip phenomena were observed for the vibrated droplets, and the time-varying contact angles were measured, which showed that in the case of vertical vibration, the left and right contact angles oscillate in-phase, whereas in the case of horizontal vibration, there is 180° phase difference between left and right contact angles. Daniel *et al*. (2001; 2002; 2004; 2005) investigated the motion of sessile liquid droplets on a solid substrate undergoing a lateral vibration, and found that a periodic force would be applied to the droplets by the vibration, which promotes the ratcheting motion of droplets by helping to overcome the contact angel hysteresis. CFD simulation by Dong *et al*. (2006) verified that the promoting effect reaches the maximum at the resonant frequencies due to the larger contact angle variation on both sides of the droplets. Mettu and Chaudhury (2011) demonstrated that finite hysteresis is necessary for a drop to move on a surface when it is subjected to a period but asymmetric vibration. They (2008) also studied the motion of drops on a surface induced by thermal gradient and vibration, and presented a simple model that describes the dependence of drop velocity on hysteresis, vibration amplitude, and resonance frequencies of vibration.

The mechanical vibration can not only promote the droplet motion on a solid substrate, but also enhance the heat and mass transfer inside the drop by inducing internal flows (Kaji *et al*., 1985; Chung and Trinh, 2000; Zhu *et al*., 2002; Kinoshita *et al*., 2007). Hao *et al*. (2010, 2011a,b) studied the dynamic transportation of a water droplet on the microstructured hydrophobic silicon substrates and obtained the internal flow pattern inside the droplet by using the particle image velocimetry (PIV) technique. It has also been demonstrated that the acoustic vibration can create fluid flow, such as streaming, microstreaming, and surface waves, and also enhance heat transfer in the thin liquid film (Eslamian, 2017). Muggele *et al*. (2006; 2011) triggered the self-excited oscillation of droplets by using electrowetting to accelerate the internal mixing of water and observed the internal flow pattern by following the motion of fluorescent dyes. They demonstrated an axisymmetric internal flow for the oscillating droplets that is first pulled downwards along the symmetry axis, and subsequently folds back upwards along the surface of the drop towards the apex. However, opposite results were obtained by Lim's group (Shin and Lim, 2014; Kim and Lim, 2015) and Park *et al*. (2016), they found that a vertically vibrating droplet attains various shapes at different modes, resulting in complicated vortices inside the droplet. In the visualization, the flow moves upwards starting from the bottom center of the droplet along the symmetric axis and then moves closer to the three phase contact line along the surface of the upper part of the droplet.

All the mentioned investigations on the internal flow inside the oscillating droplets considered the cases of sessile drops undergoing vertical vibration, while the similar studies for drop undergoing lateral vibration has not been reported. In this study, we investigated the internal flow pattern inside a sessile droplet undergoing a lateral vibration using both the experimental and computational fluid dynamic (CFD) methods. By initially staining droplet partially with fluorescent Rhodamine B, the main flow inside the vibrating droplet was analyzed by tracing the motion of the fluorescent dye. CFD simulation demonstrated that extra flow circuits exist inside the droplet besides the main flow. Moreover, fluid mixing inside the droplet was evaluated to compare the velocity of the main flow at different vibration frequencies.

2. EXPERIMENTAL

2.1 Preparation of Hydrophobic Substrates

In this study, glass slides (76 × 26 mm) treated with octadecyltrichorosilane (OTS) were used as the hydrophobic solid substrates. The glass slide was firstly ultrasonically cleaned and dried using ultrapure nitrogen gas, then immersed in hot piranha solution (30% H_2O_2, 70% H_2SO_4) for 1 hour at 90°C to remove the impurities. After being rinsed with copious amounts of distilled water, the glass slide was dried with ultrapure nitrogen gas, and then immersed in the solution of 0.1 ml of OTS in 25 ml of hexadecane and heated at 90°C in an oven for 20 minutes (Daniel *et al*., 2001). Subsequently, the wafer was treated with chloroform for 15 min and anhydrous alcohol for 30 minutes, and finally dried using ultrapure nitrogen gas (Hao *et al*., 2011). Yong's contact angle of the obtained hydrophobic solid substrate was measured to be 110±1° using a contact angle analyzer (OCA20, Dataphysics). It is noteworthy that the dry environment during the preparation is crucial for obtaining a high-quality hydrophobic surface by suppressing the reaction of silanes with the atmospheric water.

2.2 Experimental Setup

The experimental setup is illustrated in Fig. 1, in which, a YE1311B function generator (Yangzhou Radio Factory, China) was used to supply sinusoidal waves with different amplitudes and frequencies by adjusting the electrical voltages and frequencies (the frequency range used in the experiments is 90–170Hz and the amplitude is

0.1mm). A TS-ICP IEPE power conditioner (TYTEST Co. LTD, China) was connected to the substrate for determining the vibration amplitude. In order to follow the internal flow inside the oscillating droplet, two droplets of different sizes were merged during the oscillation with the top smaller one containing fluorescence (Rhodamine B) such that the top of the resulting larger droplet was stained whereas the bottom remained dark under the epifluorescence observation (Mugele *et al*., 2011). The side view video snapshots of the oscillating drop were recorded with a charge coupled device (CCD) camera (MC20-N, OLYMPUS) equipped with a SZ-61 microscope (OLYMPUS). The fluorescent light at 512 nm was supplied by a halogen lamp (CEL-350A, OLYMPUS). The whole experiment setup was placed on a vibration isolation platform to avoid the effect of external factors. It should be noted that the concentration of Rhodamine B in the droplet is very low (< 0.1%) and its particle size is very small (15 nm), it does not affect the fluid flow by closely following the fluid stream. During the experiments, the environmental humidity was controlled, and the measurements were carried out as fast as possible for minimizing the effect of droplet evaporation.

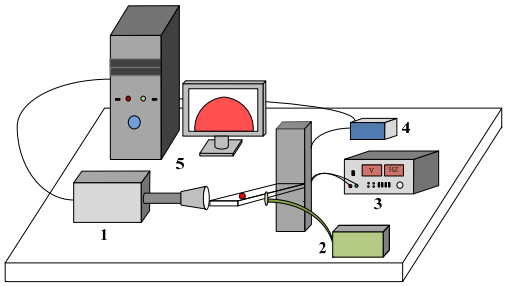

Fig. 1. Schematic of the experimental setup
1. CCD; 2. Function generator; 3. Halogen lamp; 4. IEPE power conditioner; 5. Computer

2.3 Mathematical Formulation

A FLUENT package was employed to simulate the internal flow field inside the laterally oscillating droplet, in which, the 3d Navier-Stokes and continuity equations are solved using a well-established volume of fluid (VOF) model. In this study, we only considered the cases that the contact line remains pinned when the external force could not overcome the contact angle hysteresis. In the VOF model, the continuity and Navier-Stokes equations are solved for the domains comprising two fluid phases in conjunction with an extra VOF advection equation, in which, a variable α, representing the volume fraction of one of the phases, is introduced to track the free surface. α =1 means the given computational cell is filled with one of the phases (i.e. liquid). On the contrary, α = 0 indicates that the cell is filled with the other phase (i.e. air). 0 < α < 1 denotes the cell including the interface (Daniel and Chaudhury, 2002).

The 3D Navier-Stokes equation used to solve the problem of the oscillating drop can be expressed as

$$\frac{\partial}{\partial t}(\rho \boldsymbol{v}) + \nabla \cdot (\rho \boldsymbol{v}\boldsymbol{v}) = -\nabla p + \nabla \cdot \left[\mu(\nabla \boldsymbol{v} + \nabla \boldsymbol{v}^T)\right] + \rho \boldsymbol{g} + \boldsymbol{F} \quad (1)$$

where $\boldsymbol{v}$ = (u, v, w) is the velocity vector, p is the pressure. $\rho = \alpha\rho_1 + (1-\alpha)\rho_2$ and $\mu = \alpha\mu_1 + (1-\alpha)\mu_2$ are the average density and dynamic viscosity in the computational cell. $\boldsymbol{F}$ is the volume force, being defined in the continuum surface force (CSF) model as Eq. (2) (Brackbill, Kothe and Zemach, 1992).

$$\boldsymbol{F} = \sigma \frac{\rho \kappa \nabla \alpha}{\frac{1}{2}(\rho_1 + \rho_2)} \quad (2)$$

where σ is the interfacial tension between the two phases, and κ is the interfacial curvature of the liquid phase, which can be calculated according to the outward unit normal vector $\boldsymbol{n} = \frac{\nabla \alpha}{|\nabla \alpha|}$ by Eq. (3).

$$\kappa = -\nabla \cdot \boldsymbol{n} \quad (3)$$

In the CFD simulation, the diameter of the studied liquid droplet is 2 mm and the vibration amplitude of the substrate for all the simulation is 0.5 mm. The numerical analysis was carried out on a uniform rectangular mesh with the size of 40 μm × 40 μm × 40 μm, which was selected by decreasing the mesh size until the simulation results were no longer depended on the mesh size. The boundary conditions on the solid surface are no-slip and no-penetration conditions as Eq. (4).

$$u = U_s, \quad v = 0, \quad w = 0 \quad (4)$$

In Eq. (4), U_s is the velocity of the vibrating substrate. For a sinusoidal periodic vibration, $U_s = 2\pi\omega \mathrm{A}\cos(2\pi\omega t)$, A and ω being the vibration amplitude and frequency. In our simulation, user defined function (UDF) program has been written to define U_s in FLUENT.

3. RESULT AND DISCUSSION

According to the previous studies (Brunet *et al*., 2008; 2009; Daniel *et al*., 2002; 2005), the Rayleigh resonant modes of a sessile droplet in partial contact with a substrate undergoing a lateral oscillation can still be calculated by Lamb's equation (Eq. (5)) (Wilkes and Basaran, 1997).

$$\omega = \sqrt{\frac{\gamma}{3\pi m} n(n-1)(n+2)} \quad (5)$$

where ω is the resonant frequency, n is an integer value of 2 or higher, γ and m are the surface tension and mass of the droplet, respectively. Later, Strani and Sabetta (1984) showed that a drop in partial contact with a surface has an extra low-frequency mode related to the oscillation of the center-of-

mass, which is called the rocking mode. For the water droplet with a diameter of 2 mm and mass of 3.1 mg investigated in this study, the resonant frequencies for the rocking mode and the first and second Rayleigh mode can be determined to be around 60 Hz, 140 Hz and 272 Hz, respectively (Dong *et al*., 2006).

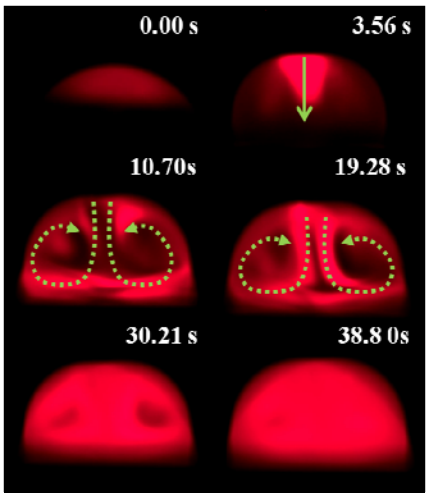

Fig. 2. Experimental visualization of the flow pattern inside a sessile water droplet on a substrate undergoing a lateral vibration. The diameter of the droplet is 2 mm and the mass is 3.1 mg. The vibration frequency is 140Hz and the amplitude is 0.1 mm. The green dotted lines are used to indicate the flow direction. The rate of the camera in the experiments is 200 frames per second.

Figure 2 demonstrated the flow pattern inside a sessile water droplet undergoing a lateral vibration, indicted by the redistribution of Rhodamine B inside the droplet. Once the droplet starts to oscillate, the stained fluid containing the fluorescence on the top flows downward from the center, and then flows upwards near the surfaces to form two counterflow circuits, resulting in the uniform distribution of Rhodamine B inside the droplet within a few seconds depending on the viscosity of the droplet liquid. This result agrees with that obtained by Muggele *et al*. (2006; 2011) for the cases of electrowetting-triggered vertically oscillating droplets, in which, the fluid first pulled downwards along the symmetry axis, and subsequently moves upwards along the surface of the droplets.

For investigating the effect of fluid viscosity, Fig. 3 illustrated the captured images of the internal flow pattern of four droplets, whose viscosity was varied by adding different amount of glycerol to the water droplet (volume content = 5%, 10%, 20%, 40%). It was observed that the overall scenario of fluid flow inside the droplet with different viscosity is similar, with the main flow being that fluid flows downward along the central axis and ascends upward along the surface. However, for the droplet with the volume content of glycerol = 40%, two small flow circuits can be observed near the substrate.

For the sessile droplet on a laterally vibrating substrate, the substrate momentum diffuses within the Stokes layer over a distance of $(2\mu/\rho\omega)^{1/2}$. Above this distance, the droplet experiences the inertial force, while within the Stokes layer, the viscous fluid cannot be neglected. The case of the vertically vibrating droplet is different, in which, the whole droplet experiences the inertial force and the viscous force can be neglected. In this regard, the study of the internal flow inside a laterally oscillating droplet have to consider the flow within and outside the stokes layer. In the experimental study, we cannot clearly see the flow inside the Stokes layer when the fluid viscosity is low. While with an increase in fluid

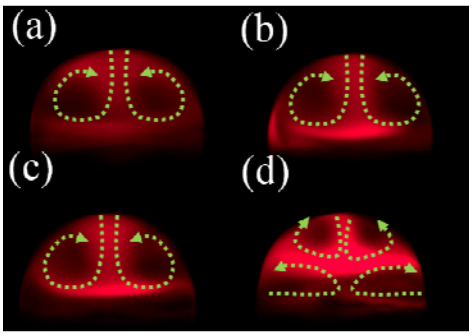

Fig. 3. Flow pattern inside a sessile water droplet with different viscosity on a substrate undergoing a lateral vibration. (a) Volume content of glycerol is 5%, vibration frequency is135 Hz, viscosity is about 1.01 cP; (b) Volume content of glycerol is 10%, vibration frequency is 135 Hz, viscosity is about 1.31 cP; (c) Volume content of glycerol is 20%, vibration frequency is 130 Hz, viscosity is about 1.76 cP; (d) Volume content of glycerol is 40%, vibration frequency is 125 Hz, viscosity is about 4.86 cP; The vibration amplitude is 0.1 mm and the green dotted lines are used to indicate the flow direction.

viscosity, the Stokes layer becomes thicker and the flowing speed becomes slower; two small flow circuits were observed near the bottom boundary in Fig. 3d.

To further clarify the flow pattern inside the oscillating droplet, the internal velocity vector distribution and flow streamline were investigated by using the CFD method. It can be seen from Fig. 4 that at all the three resonant modes, the flow pattern inside the droplet has multiple flow circuits with the main flow being the downstream along the central axis. Besides the main flow, two counterflow circuits, induced by the Laplace force due to the droplet deformation, can be observed inside both sides of the drop. During the lateral oscillation, the fluid inside the droplet experiences an inertial force, which causes the drop to deform. The deformation is associated with an increase of the surface area of the drop and the variation of the local curvature along the drop surface. Accordingly, a restoring force arises inside the deformed drop due to the Laplace pressure, which attempts to decrease the surface area and restore the drop to its original shape. Competition

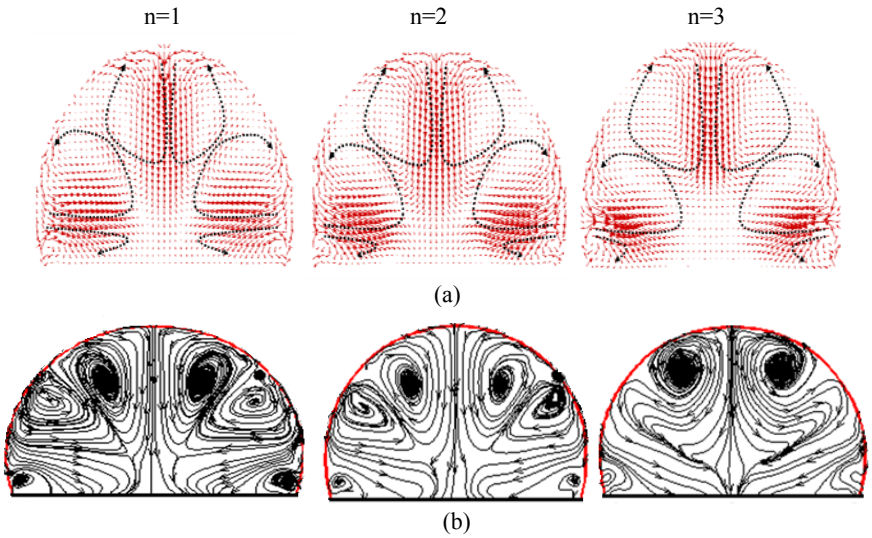

Fig. 4. CFD simulation result of a laterally vibrating water droplet at the resonance modes. (a) Distribution of internal velocity vector; (b) Internal flow streamline. The first mode (n=1) corresponds to the rocking mode, and the second and third modes here corresponds to the Rayleigh first and second modes. The velocity vector and streamline images were obtained by using the software of TECPLOT to process the simulation data of FLUENT.

between the inertial force and Laplace force causes capillary waves appearing on the free surface, resulting the different shpes of the droplet at various resonant modes, and two internal counter-current flow circuits arise inside both side of the droplet. Moreover, inside the oscillating droplet, two flowing circuits appear inside the Stokes layer near the bottom substrate, resulted by the diffusion of substrate momentum within the Stokes layer. Since the Stokes layer region $(2\mu/\rho\omega)^{1/2}$ becomes thinner with an increase in the vibrating frequency, the two circuits near the substrate turn weaker from the first resonant mode (n=1) to the third resonant mode (n=3).

For comparing the velocity of the internal flow inside the oscillating droplet, especially the main flow, we analyzed the experimental merging time of vibrating droplets at different frequencies. The merging time refers to the time that the droplets start to oscillate (the image at 0.00s in Fig. 2) to the time that Rhodamine B is uniformly dispersed in the droplet (the image at 38.80 s in Fig. 2). As showed in Fig. 5, the merging time for the droplets with different viscosity varies with the vibrating frequencies. As anticipated, the minimum merging time occurs at the resonant frequency, demonstrating that the main flow inside the oscillating droplet is faster at the resonant mode. For the droplet undergoing a lateral vibration, the inertial force experienced by the drop is balanced by the hydrostatic (pressure) and viscous force, while the hydrostatic force exhibits minima at the resonant frequencies, resulting in the maximum deformation of the oscillating droplet, which is accompanied by the faster internal flow inside the droplet. Figure 5 also shows that the merging time increases with an increase in liquid viscosity, but the resonant frequency decreases with an increase in liquid viscosity due to the decreased surface tension (the value of the surface tension is 0.073N/m, 0.071N/m, 0.067N/m, 0.063N/m, 0.056N/m respectively with the increase of the liquid viscosity.).

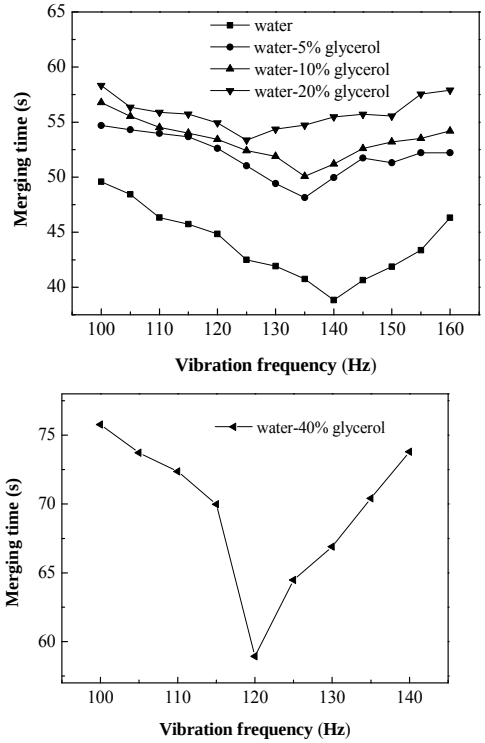

Fig. 5. Experimental merging time for vibrating droplets at different frequencies

4. CONCLUTION

In this study, the internal flow of a droplet standing on a hydrophobic substrate undergoing a lateral vibration was analyzed by using both experimental and CFD simulation method. By initially staining

droplet partially with fluorescent Rhodamine B, we found the main flow inside the oscillating drop is the fluid flows downward along the central axis and ascends upward along the surface to form two main flowing circuits. The CFD simulation using the VOF-CSF model demonstrated that extra four flow circuits exits inside the laterally oscillating droplet besides the main flow. The diffusion of substrate momentum within the Stokes layer results in the two flow circuits near the bottom substrate, and the Laplace force due to the droplet deformation induces the two counter-current flow circuits near the surface inside both side of the droplet. Moreover, the velocity of internal flow inside the oscillating droplet is investigated by evaluating the mixing time of the partially staining droplet, which demonstrated that the main flow inside the oscillating droplet is faster at the resonant mode. Different from the previous studies (Ding *et al*., 2009; Celestini and Kofman, 2006) that focused on the movement mechanism and shape revolution of a laterally vibrated droplet mainly from the macro perspective, this study offers a preliminary look on the internal flow pattern of a droplet undergoing a lateral vibration from a micro perspective.

ACKNOWLEDGMENTS

This work was financially supported by the National Science Foundation of China (21606026, 21776025), the Fundamental Research Funds for the Central Universities (106112016CDJXZ228803) and Graduate Scientific Research and Innovation Foundation of Chongqing, China (Grand NO. CYS16014).

REFERENCES

Brackbill, J. U., D. B. Kothe and C. Zemach (1992). A Continuum Method for Modeling Surface Tension. *Journal of Computational Physics* 100(2), 335-354.

Brunet, P., J. Eggers and R. D. Deegan (2008). Vibration-induced climbing of drops. *Physical Review Letters* 99(14), 144501.

Brunet, P., J. Eggers and R. D. Deegan (2009). Motion of a drop driven by substrate vibrations. *The European Physical Journal - Special Topics* 166, 11-14.

Celestini, F. and R. Kofman (2006). Vibration of submillimeter-size supported droplets. *Physical Review E* 73(4), 235-245.

Chung, S. K. and E. H. Trinh (2000). Internal flow of an electrostatically levitated droplet undergoing resonant shape oscillation. *Physics of Fluids* 12(2), 249-251.

Daniel, S., M. K. Chaudhury and J. C. Chen (2001). Past drop movements resulting from the phase change on a gradient surface. *Science* 291(5504), 633-636.

Daniel, S. and M. K.Chaudhury (2002). Rectified motion of liquid drops on gradient surfaces induced by vibration. *Langmuir* 18(9), 3404-3407.

Daniel, S., S. Sircar, J. Gliem and M. K. Chaudhury (2004). Ratcheting motion of liquid drops on gradient surfaces. *Langmuir* 20(10), 4085-4092.

Daniel, S., M. K. Chaudhury and P. G. de Gennes (2005). Vibration-actuated drop motion on surfaces for batch microfluidic processes. *Langmuir* 21(9), 4240-4248.

Daw, R. and J. Finkelstein (2006). Lab on a chip. *Nature* 442(7101), 367-367.

Ding, Z. W., W. B. Song and B. Ziaie (2009). Sequential droplet manipulation via vibrating ratcheted microchannels. *Sensor and Actuators B-Chemical* 142(1), 362-368.

Dong, L., A. Chaudhury and M. K. Chaudhury (2006). Lateral vibration of a water drop and its motion on a vibrating surface. *The European Physical Journal E* 21(3), 231-242.

Eslamian, M. (2017). Excitation by acoustic vibration as an effective tool for improving the characteristics of the solution-processed coatings and thin films. *Progress in Organic Coatings* 113, 60-73.

Hao, P. F., C. J. Lv, Z. H. Yao and F. He (2010). Sliding behavior of water droplet on superhydrophobic surface. *Science China-Physics Mechanics & Astronomy* 55(12), 66003-66008.

Hao, P. F., C. J. Lv, X. W. Zhang, Z. H. Yao and F. He (2011a). Driving liquid droplets on microstructured gradient surface by mechanical vibration. *Chemical Engineering Science* 66 (10), 2118-2123.

Hao, P. F., Z. H. Yao and X. W. Zhang (2011b). Study of dynamic hydrophobicity of microstructured hydrophobic surfaces and lotus leaves. *Science China-Physics Mechanics & Astronomy* 54(4), 675-682.

Kaji, N., Y. H. Mori and Y. Tochitani (1985). Heat-Transfer Enhancement Due to Electrically Induced Resonant Oscillation of Drops. *Journal of Heat Transfer-Transactions of the Asme* 107(4), 788-793.

Kelvin, B. (1882). *Mathernatical and Physical Paper*. Cambridge University Press: New York.

Kim, H. and H. C. Lim (2015). Mode Pattern of Internal Flow in a Water Droplet on a Vibrating Hydrophobic Surface. *The Journal of Physical Chemistry B* 119(22), 6740-6746.

Kinoshita, H., S. Kaneda, T. Fujii and M. Oshima (2007). Three-dimensional measurement and visualization of internal flow of a moving droplet using confocal micro-PIV. *Lab on a Chip* 7(3), 338-346.

Lamb, H. (1932). *Hydrodynamics*. Cambridge University Press: UK.

Lee, Y. R., J. H. Shin, I. S. Park, K. Rhee and S. K.

Chung (2015). Energy harvesting based on acoustically oscillating liquid droplets. *Sensors and Actuators A-Physical* 231, 8-14.

Mettu, S. and M. K. Chaudhury (2001). Motion of liquid drops on surfaces induced by asymmetric vibration: role of contact angle hysteresis. *Langmuir* 27(16), 10327-10333.

Mettu, S. and M. K. Chaudhury (2008). Motion of drops on a surface induced by thermal gradient and vibration. *Langmuir* 24(19), 10833-10837.

Moon, J. H., B. H. Kang and H. Y. Kim (2006). The lowest oscillation mode of a pendant drop. *Physics of Fluids* 18(2), 180.

Mugele, F., J. C. Baret and D. Steinhauser (2006). Microfluidic mixing through electrowettinginduced droplet oscillations. *Applied Physics Letters* 88(20), 204106.

Mugele, F., A. Staicu and R. Bakker (2011). Capillary Stokes drift: a new driving mechanism for mixing in AC-electrowetting. *Lab on a Chip* 11(12), 2011-2016.

Noblin, X., A. Buguin and F. Brochard-Wyart (2009a). Vibrations of sessile drops. *The European Physical Journal-Special Topics* 166, 7-10.

Noblin, X., R. Kofman and F. Celestini (2009b). Ratchetlike motion of a shaken drop. *Physical Review Letters* 102(19), 194504.

Park, C. S., H. Kim and H. C. Lim (2016). Study of internal flow and evaporation characteristics inside a water droplet on a vertically vibrating hydrophobic surface. *Experimental Thermal and Fluid Science* 78, 112-123.

Rahimzadeh, A. and Eslamian M. (2017). Experimental study on the evaporation of sessile droplets excited by vertical and horizontal ultrasonic vibration. *International Journal of Heat & Mass Transfer*, 114, 786-795.

Rayleigh, L. (1894) *The Theory of Sound*. Macmillan: UK.

Shin, Y. S. and H. C. Lim (2014). Shape oscillation and detachment conditions for a droplet on a vibrating flat surface. *The European Physical Journal E* 37(8), 1-10.

Strani, M. and F. Sabetta (1984). Free-Vibrations of a Drop in Partial Contact with a Solid Support. *Journal of Fluid Mechanics* 141, 233-247.

Wilkes, E. D. and O. A. Basaran (1997). Forced oscillations of pendant (sessile) drops. *Physics of Fluids* 9(6), 1512-1528.

Zhu, J. H., F. Zheng, M. L. Laucks, and E. J. Davis (2002). Mass transfer from an oscillating microsphere. *Journal of Colloid and Interface Science* 249(2), 351-358.